Adsorption and Desorption of Emerging Water Contaminants on Activated Carbon Fabrics

Sandrine Delpeux-Ouldriane[1], Mickaël Gineys[1], Nathalie Cohaut[1], François Béguin[1], Sylvain Masson[2], Laurence Reinert[2], Laurent Duclaux[2]
[1]CNRS-Université d'Orléans, ICMN
1B Rue de la Férollerie, Orléans, France, 45071
delpeux@cnrs-orleans.fr
[2]Université Savoie Mont Blanc, LCME
Chambéry, France, 73000
laurent.duclaux@univ-savoie.fr

Abstract - *Nowadays, a wide variety of organic contaminants is present at trace concentrations in wastewater effluents. In order to mitigate these pollution problems, the implementation of the REACH European regulation has defined lists of targeted pollutants to be eliminated selectively in water. This therefore implies the development of innovative and more efficient remediation techniques. In this regard, adsorption processes can be successfully used to achieve the removal of organic compounds in waste water treatment processes, especially at low pollutant concentration. Activated carbons possess a highly developed porosity and thus demonstrate high adsorption capacities. More specifically, carbon cloths show high adsorption rates, ease of handling, good mechanical integrity and regeneration potential. When loaded with pollutants, these materials can be regenerated using electrochemical polarization.*

Keywords: Nanoporous carbons, activated carbon cloths, adsorption, micropollutants, emerging contaminants, regeneration, electrochemistry.

1. Introduction

A wide variety of organic compounds that are used in domestic, agricultural and industrial applications are present at trace concentrations in wastewater effluents [1, 2]. These micropollutants include personal-care products, plasticizers, reproductive hormones, pesticides and pharmaceuticals [3]. The adsorption properties of activated carbons offer great potential for water purification, particularly in the case of tertiary treatments as they are the most prevalent and competitive adsorbents, especially at low pollutant concentration. However, the major disadvantage encountered is their short lifetime due to the low and expensive regeneration capacities. Generally, the loaded carbon adsorbent can be regenerated *ex-situ* through high energy-consuming processes, like thermal treatments or steaming.

Specifically, as compared to powder or granules, activated carbon cloths (ACC) show numerous advantages, thanks their ease of handling, high mechanical integrity and regeneration potential. Additionally, due to their microtexture and their small fiber diameters (around 10 μm), they are ideal candidates for adsorption purposes as they show minimal diffusion limitation and greater adsorption rates towards noxious organic pollutants [4].

In the present work, the adsorption properties of some micropollutants and emerging pollutants, especially pharmaceutical residues, were investigated using an activated carbon cloth. Electrochemical polarization was applied to achieve the reversible desorption of adsorbed species and the regeneration of the adsorbent porosity [5, 6].

The involved mechanisms were carefully examined and correlated to the nanoporous texture of the adsorbent by taking into account the adsorbate speciation and physico-chemical properties. Results

1

show that the reversible electrochemical desorption of the induced charged molecules offers great promise. Such systems could find a place of choice in industrial processes for tertiary treatment and for the treatment of hospital effluents, but also for underground water exploitation [7].

2. Experimental

2. 1. Adsorbent

An activated carbon cloth possessing a highly developed surface area was used (Table 1). Its porous network consisted of a large amount of supermicropores (0.7-2 nm) and ultramicropores (< 0.7 nm). The pore size distribution was very narrow and centered at 1-1.2 nm.

Table 1. Microtextural adsorbent characteristics.

S_{BET} (m^2/g)	V_{MICRO} N_2, DFT (cm^3/g)	V_{MESO} N_2, DFT (cm^3/g)	V_{MICRO} N_2, DR (cm^3/g)	V_{MICRO} CO_2, DR (cm^3/g)	V_{TOTAL} N_2 (cm^3/g)
1175	0.59	0.09	0.57	0.57	0.68

This material was rather hydrophobic and contained 95 % (mass %) of carbon and 1.2% of oxygen. It presented a basic zero charge pH (8.9) and a low amount of oxygenated surface groups (0.2 mmol/g).The diameters of the fibers were in the range of ten micrometers and micropores were directly accessible all along the fibers (Figure 1).
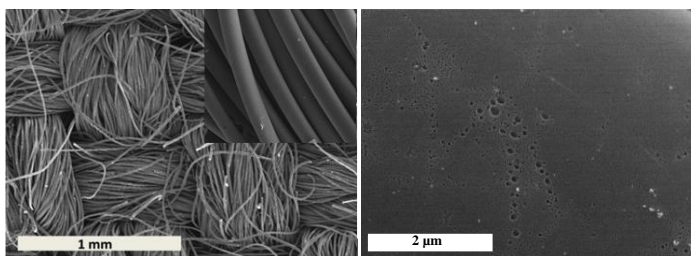

Figure 1. SEM images of the activated carbon cloth.

2. 2. Targeted Pollutants

Seven organic molecules, diclofenac (DFN), caffeine (CAF), acetaminophen (also called paracetamol POL), bisphenol A (BPA), carbamazepine (CBZ), pentachlorophenol (PCP) and ofloxacin (OFX) were selected (Figure 2).

These contaminants possess different physico-chemical properties: water solubility, polarity, pK_A values, and molecular volumes (Table 2).
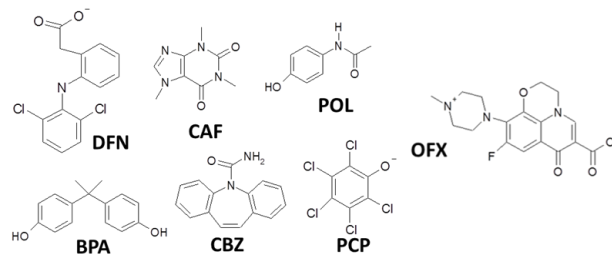

Figure 2. Adsorbates formulae and speciations at pH 7.5.

Table 2. Pollutants characteristics at pH7.5.

	pK_{A1} / pK_{A2}	V ($Å^3$)	s (mmol/L)	Log K_{ow}
POL	9.5	138	74.0	1.08
PCP	5.0	144	5.7	1.90
CAF	0.6	340	225.2	-0.79
CBZ	2.3/13.9	400	0.2	3.22
BPA	9.8	460	0.7	4.32
DFN	4.0	580	154.1	0.55
OFX	5.5/8.2	850	144.5	-0.93

2. 3. Analytical Detection and Quantification

Reverse phase HPLC was used to perform the detection and the quantification during adsorption kinetics, in binary or complex mixture and isotherm adsorption. The chromatographic separation was performed in the reversed phase mode using a Hypersil Gold C_{18} column at 25°C (100 × 2.1 mm with a particle size of 3 μm). The eluents were water (A) at pH 2.9 through acidification by orthophosphoric acid 0.01 % (v/v) and acetonitrile (B). The following multi-step linear gradient was applied: from 10 % B to 80 % B in 25.45 min (slope of 2.75 mL/min), followed by a plateau for 2 min then a decrease from 80 % B to 10 % B in one minute and a final plateau of 3 min at the initial conditions. The flow rate was set to 0.25 ml/min and the volume of injection to 50 μL [8].

2. 4. Adsorption Measurements

All the kinetics studies were conducted in a phosphate buffer at pH 7.5. In the case of binary mixtures, a total concentration of 10^{-4} mol/L was set (5.10^{-5} mol/L per each pollutant). For the complex mixture, a total concentration of 10^{-4}mol/L was set ($1.43.10^{-5}$ mol/L per each pollutant). The kinetics data were fitted with the pseudo second order model.

The adsorption isotherms were studied at 13, 25 and 40°C for DFN, CAF, CBZ, BPA and OFX. Experimentally, stoppered vials containing disks of carbon adsorbent (12 mg) were placed in 50 mL pollutant solution at various concentrations (from

about 10^{-5} to 10^{-3} mol/L) and stirred until equilibrium was reached. The equilibrium time was strongly dependent of the pollutants nature. For some molecules, seven days were sufficient, except for OFX (21 days), DFN (14 days) and PCP (10 days). The solutions prepared at a given concentration were exactly the same for each of the three temperatures in order to obtain precise and comparable results. The solutions were filtered on 0.45 μm filter membranes prior to HPLC analysis.

2. 5. Regeneration Under Polarization

Regeneration was performed using a classical three electrode system connected to a galvanostat/potentiostat (VMP-1, Biologic) in a 0.01 mol.L^{-1} Na_2SO_4 electrolyte (pH = 5.9 and σ = 2.5 mS.cm^{-1}). After adsorption in open circuit voltage (OCV), the loaded ACC disk was washed with ultra-pure water (σ_{water} = 0,055 μS.cm^{-1}) and attached to a current collector for the electro-desorption experiments. A counter electrode and Hg/Hg_2SO_4 (E = 0.649 V *vs* NHE) as reference electrode were used. Negative currents (-10 mA) were applied to the activated carbon cloth electrode [7, 9].

3. Results and Discussion

3. 1. Adsorption Isotherms

Isotherms were studied at 298 K (not shown) in order to calculate the Gibbs free energy variation ΔG^0_{298K} at a maximum uptake for the adsorption of five molecules on the carbon fabric (Table 3). All the isotherms except that of OFX were simulated using the Langmuir-Freundlich equation Eq. 1 as:

$$Q_e = Q_{max} \times (K_{lf} C_e)^n / (1 + (K_{lf} C_e)^n \qquad (1)$$

where Q_e is the adsorption uptake at equilibrium (mmol/g), C_e is the concentration at equilibrium (mmol/L), k_{lf} is the Langmuir-Freundlich constant (L/mmol), Q_{max} is the maximum uptake (mmol/g) and n is the Langmuir-Freundlich exponent.

The OFX and BPA isotherms were better simulated by a Langmuir model for which the n exponent values were equal to one in the previous equation (Table 2).

The Gibbs free energy variations ΔG^0_{298K} were determined from Eq. 2 as:

$$\Delta G^0_T = -RT \ln (K) \qquad (2)$$

where R is the ideal gas constant, T the temperature (K) and K the equilibrium constant (estimated from the relation $K = C_{ads}/C_e$, where C_{ads} is the concentration adsorbed at equilibrium in mmol/L).

In order to compare the ΔG^0_{298K} values of the different adsorbates, they were calculated at the Q_e uptake value equal to 80% of Q_{max} for each isotherm. Negative and small ΔG^0 showed a spontaneous and physical adsorption process. ΔG^0 values are discussed in section 3.2 where it is shown that the thermodynamic process is the dominant process for long adsorption time kinetics.

Table 3. Gibbs free energy for different micropollutants at a maximum uptake and Langmuir-Freundlich parameters of the isotherms at 298 K.

	OFX	DFN	BPA	CBZ	CAF
ΔG^0 (kJ/mol)	-17.5	-14.6	-13.5	-10.2	-0.7
Q_{max} (mmol/g)	0.7	1.35	1.72	1.59	1.9
Q_{max} (mg/g)	253	400	393	376	369
K_{lf} (L/mmol)	14930	7051	9612	2828	820
n	1	1.12	1	1.15	0.85

3. 2. Adsorption Kinetics

In order to understand the adsorption mechanisms and to determine the key parameters governing adsorption, kinetics studies in binary or complex mixtures were performed. In some cases, competition effects were clearly visible as for example between DFN and CAF and between DFN and POL. Two regimes were detected: during the first five days the speciation and hydrodynamic volume of the adsorbates controlled the adsorption kinetics, with anionic adsorbates being adsorbed more slowly because of electrostatic repulsions. In a second step for longer times, polarity and therefore water solubility governed the adsorption uptake, with the less soluble and most hydrophobic DFN becoming easier to adsorb onto the hydrophobic carbon adsorbent surface (Figure 3 and Figure 4).

When approaching equilibrium, the adsorption of DFN occurred to the detriment of CAF or POL molecules, thus demonstrating that these molecules were in competition for some adsorption sites and that when DFN entered the pores, POL or CAF were removed from the pores. The molecules of CAF with a weak Gibbs energy of adsorption (ΔG^0_{abs}) were desorbed from some of their adsorption sites and replaced by the competing

contaminants (DFN) interacting at lower energy with the ACC.

The adsorption behavior of DFN in the different binary systems showed that its adsorption capacity and adsorption kinetic were affected to a different extent. Firstly, one must consider the large size of the DFN molecule, in the range of 580 Å3, as compared to the smaller molecules such as POL, PCP and CAF. More precisely, adsorbed DFN uptake was lowered especially when DFN was co-adsorbed with large species such as OFX and BPA (Figure 5 and Table 4).
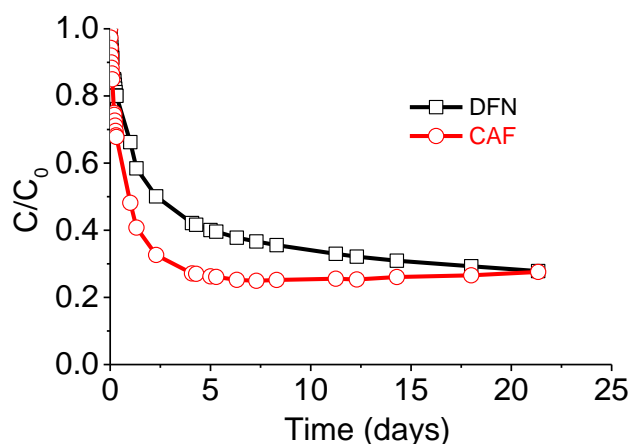

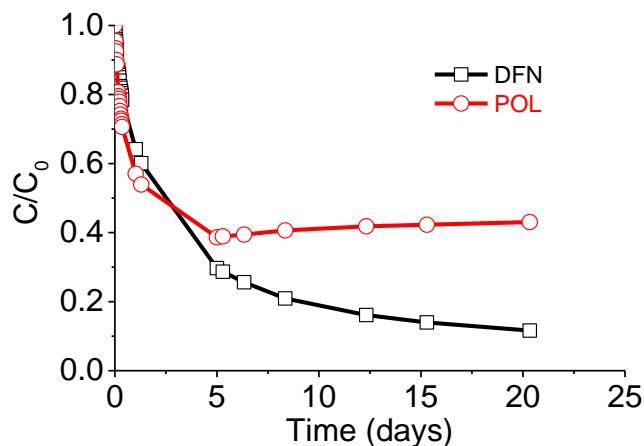Figure 3. Adsorption of DFN and CAF (kinetics data).

Figure 4. Adsorption of DFN and POL (kinetics data).

For co-adsorbates having the smallest hydrodynamic volumes, such as POL or CAF, the amounts of DFN adsorbed were less affected and high adsorption uptakes were measured.

These results showed the major role of adsorbate size during adsorption processes. For two adsorbates having different volumes, each of them could easily find an adsorption site in the porosity. For molecules that

are large compared to the small size of the pores, it became more complicated, and adsorbates were in competition to reach the bigger micropores (Figure 6).
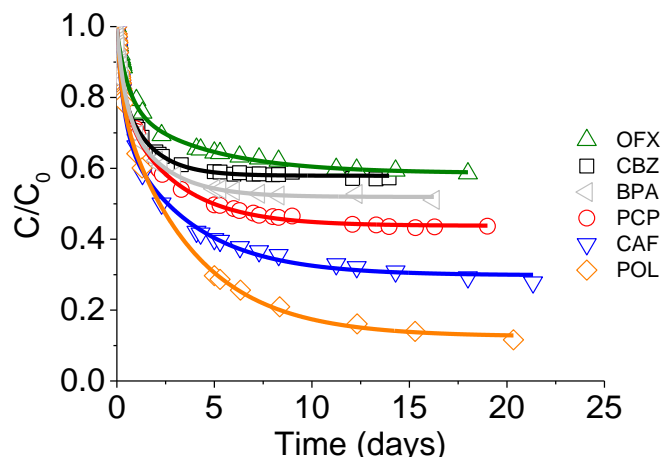

Figure 5. Adsorption kinetics of DFN in binary systems depending on the co-adsorbate.

Table 4. DFN adsorption characteristics.

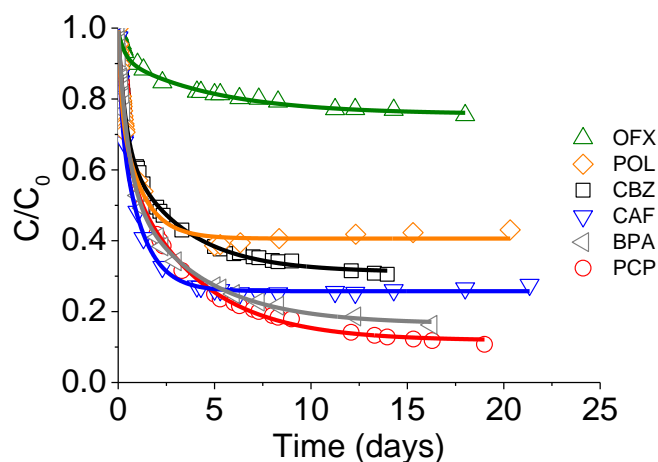| Co-adsorbate	Q_{ads} DFN mmol/g	Q_{ads} Co-adsorbate mmol/g
POL	1.03	0.70
PCP	0.69	1.07
CAF	0.82	0.90
CBZ	0.51	0.82
BPA	0.60	0.96
OFX	0.49	0.27

Figure 6. Adsorption kinetics of the co-adsorbate in binary systems with DFN.

When the adsorption kinetics were studied in a complex mixture containing the seven adsorbates, the same tendency was observed. The adsorbate size appeared to be the main parameter controlling the adsorption kinetics. The highest adsorption capacities

were observed for the smallest organic molecules such as PCP and POL, whereas OFX and DFN which are large anionic molecules showed the slowest adsorption and the smallest uptake (Figure 7). The adsorption capacities could thus be directly correlated to the volume of the adsorbates.
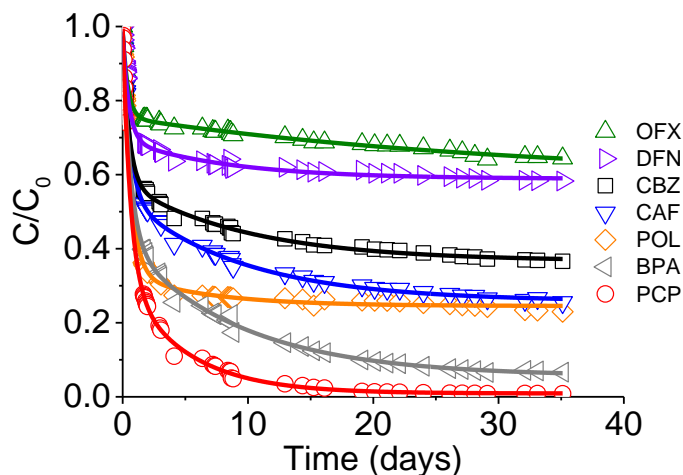

Figure 7. Adsorption kinetics of each pollutant in the complex mixture.

In order to complete the work, additional binary systems were studied with OFX in binary mixture and five co-adsorbates (PCP, BPA, DFN, CAF and CBZ). Like DFN, OFX was poorly adsorbed in the presence of PCP and BPA in the mixture (Table 5).

Table 5. OFX adsorption characteristics.

Co-adsorbate	Q_{ads} OFX mmol/g	Q_{ads} Co-adsorbate mmol/g
DFN	0.11	0.40
BPA	0.11	0.75
CBZ	0.26	1.02
CAF	0.41	0.95
PCP	0.09	0.94

OFX adsorption uptake at equilibrium was higher in the mixture with small molecules such as CAF and CBZ. Moreover, CAF single adsorption showed greater ΔG^0 than other molecules because of their small affinity with the carbon. The size effect was confirmed to be a key parameter driving the adsorption process in a binary system. Large molecules such as DFN and BPA diffused slowly into the pores because of steric hindrance whereas small molecules such as PCP and CAF diffused more rapidly and deeply inside the pores (Figure 8).

3. 3. Regeneration Under Polarization

After loading activated carbon cloths with organic contaminants, an attempt at regeneration was conducted under cathodic polarization of the carbon cloth. Depending on the nature on the adsorbate, it was possible to perform the reversible desorption of the adsorbed species. Desorption was assumed to be performed through electrostatic repulsions occurring between the negatively charged carbon surface and the dissociated organic molecules, reinforced by the presence of the electrical field. High regeneration efficiency of about 60 % was observed in the case of POL whereas for BPA (8.1 %) or DFN (11.5 %) desorption was more difficult (Figure 9).
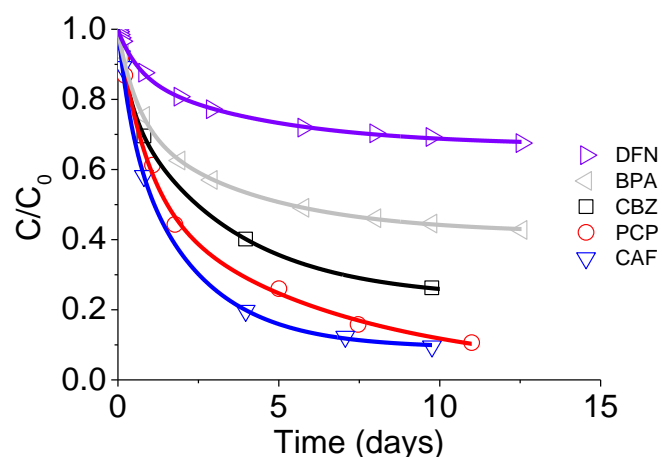

Figure 8. Adsorption kinetics of the co-adsorbates in binary systems with OFX.
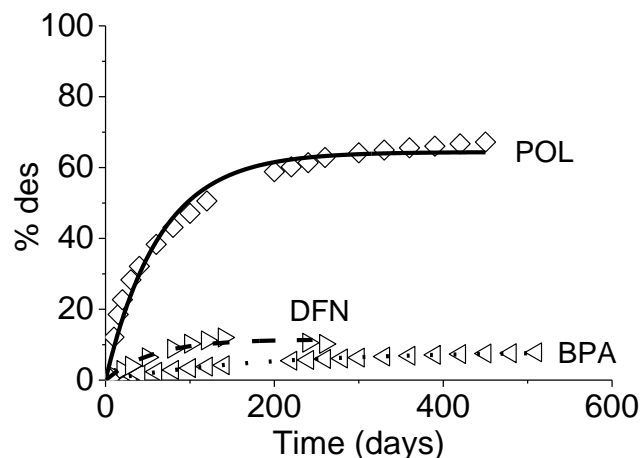

Figure 9. Regeneration percentages (%) as a function of polarization time for POL, BPA and DFN.

It was assumed that for small adsorbates as POL reversible desorption became more easy, especially

because of a better diffusion of the molecule inside the narrow pores (< 0.7nm). The incomplete regeneration was explained by either some steric blockage, especially for large molecules (DFN and BPA), inside the narrow pores or the trapping of the molecule in high energetics sites.

4. Conclusion

Activated carbon cloths are one of the most prevalent adsorbents able to trap emerging water contaminants. High adsorption capacities ranging from 250 to 400 mg/g were reached. The pollutants are mainly adsorbed in the narrow porosity by π-π interactions. In two or seven-components systems, the adsorption kinetics of pollutants (CBZ, OFX, CAF, BPA, DFN, PCP and POL) studied at 10^{-4} mol.L^{-1} on a microporous activated carbon cloth was found to be related to the molecular volume. In contrast, the solubility and the pollutant polarity were involved to a lesser extent. Small neutral molecules indeed showed the best adsorption capacities. Knowledge of the thermodynamic parameters such as ΔG^0 proved to be a useful tool to assess to what extent a molecule had been well adsorbed in a binary mixture at equilibrium. Furthermore, competition effects were highlighted. Molecules showing less negative Gibbs adsorption energy variation (ΔG°_{ads}) were desorbed from some of their adsorption sites and replaced by the competing contaminants adsorbed with lower Gibbs energy variation. The adsorbent was partially regenerated through cathodic polarization. Steric blockages by large molecule sometimes take place and make the regeneration of the material more difficult to achieve.

References
[1] M. Huerta-Fontela, M. T. Galceran, J. Martin-Alonso and F. Ventura, "Occurrence of psychoactive stimulatory drugs in wastewaters in north-eastern Spain," *Science of the Total Environment*, vol. 397, pp. 31-40, 2008.

[2] C. Stavrakakis, R. Colin, C. Faur, V. Héquet and P. Le Cloirec, "Analysis and behaviour of endocrine disrupting compounds in wastewater treatment plant," *European Journal of Water Quality*, vol. 39, no. 2, pp. 145-156, 2008.

[3] S. Snyder, C. Lue-Hing, J. Cotruvo, J. E. Drewes, A. Eaton, R. C. Pleus and D. Schlenk, *Pharmaceuticals in the Water Environment,* Report from NACWA and Association of Metropolitan Water Agencies: 2010.

[4] H. Guedidi, L. Reinert, J. M. Lévêque, Y. Soneda, N. Bellakhal and L. Duclaux, "Adsorption of ibuprofen from aqueous solution on chemically surface-modified activated carbon cloths," *Carbon*, vol. 54, pp. 432-443, 2013.

[5] C. O. Ania and F. Béguin, "Mechanism of adsorption and electrosorption of bentazone on activated carbon cloth in aqueous solutions," *Water Research*, vol. 41, pp. 3372-3380, 2007.

[6] S. Delpeux-Ouldriane, N. Cohaut and F. Béguin, "Electrochemical Removal of Ionogenic Pesticides Adsorbed on Activated Carbon Textiles," in *Proceedings of the Annual World Conference on Carbon*, Biarritz, France, 2009. vol. 3, pp. 1777-1784.

[7] S. Delpeux-Ouldriane and F. Béguin, "On Carbon Capture Reversible Assets," French Patent 1257895, August 20, 2012.

[8] M. Gineys, T. Kirner, N. Cohaut, F. Béguin and S. Delpeux-Ouldriane, "Simultaneous determination of pharmaceutical and pesticides compounds by reversed phase high pressure liquid chromatography," *Journal of Chromatography and Separation Techniques,* vol. 6, no. 6, 2015.

[9] S. Delpeux-Ouldriane, M. Gineys, N. Cohaut and F. Béguin, "The role played by local pH and pore size distribution in the electrochemical regeneration of carbon fabrics loaded with bentazon," *Carbon*, vol. 94, pp. 816-825, 2015.